

Strain-induced anticrossing of bright exciton levels in single self-assembled GaAs/Al_xGa_{1-x}As and In_xGa_{1-x}As/GaAs quantum dots

J. D. Plumhof,^{1,*} V. Křápek,² F. Ding,^{1,3} K. D. Jöns,⁴ R. Hafenbrak,⁴ P. Klenovský,² A. Herklotz,⁵ K. Dörr,⁵ P. Michler,⁴ A. Rastelli,^{1,†} and O. G. Schmidt¹

¹*Institute for Integrative Nanosciences, IFW Dresden, Helmholtzstrasse 20, D-01069 Dresden, Germany*

²*Institute of Condensed Matter Physics, Masaryk University, Kotlářská 2, CZ-61137 Brno, Czech Republic*

³*Key Laboratory of Semiconductor Materials Science, Institute of Semiconductors, Chinese Academy of Sciences, Beijing 100083, China*

⁴*Institut für Halbleitertechnik und Funktionelle Grenzflächen, University of Stuttgart, Allmandring 3, D-70569 Stuttgart, Germany*

⁵*Institute for Metallic Materials, IFW Dresden, Helmholtzstrasse 20, D-01069 Dresden, Germany*

(Received 7 February 2011; published 9 March 2011)

We study the effect of elastic anisotropic biaxial strain, induced by a piezoelectric actuator, on the light emitted by neutral excitons confined in different kinds of epitaxial quantum dots. We find that the light polarization rotates by up to $\sim 80^\circ$ and the fine structure splitting (FSS) varies nonmonotonically by several tens of μeV as the strain is varied. These findings provide the experimental proof of a recently predicted strain-induced anticrossing of the bright states of neutral excitons in quantum dots. Calculations on model dots qualitatively reproduce the observations and suggest that the minimum reachable FSS critically depends on the orientation of the strain axis relative to the dot elongation.

DOI: [10.1103/PhysRevB.83.121302](https://doi.org/10.1103/PhysRevB.83.121302)

PACS number(s): 78.67.Hc, 78.20.hb, 81.07.St, 81.07.Ta

Semiconductor quantum dots (QDs) obtained by epitaxial growth are receiving much attention because of their potential use as building blocks for quantum information processing and communication devices.^{1–7} QDs confine the motion of charge carriers in three dimensions and are thus referred to as artificial atoms. Similar to real atoms, external electric and magnetic fields can be used to manipulate the properties of bound states in QDs.^{8–13} In addition, the solid-state character of QDs allows for engineering methods which are not available for atoms. Dynamic stress fields^{14–17} represent an example, whose wide potential is only recently being recognized.^{18,19}

The emission of neutral excitons confined in QDs with symmetry lower than D_{2d} is typically split by several tens of μeV because of the anisotropic electron-hole exchange interaction.^{9,20,21} This broken degeneracy of the bright excitonic states, referred to as fine structure splitting (FSS), prevents the use of QDs as sources of entangled photon pairs on demand.^{4–7,22} External electric or magnetic fields have been applied to restore the QD symmetry and achieve FSS values comparable to the radiative linewidth.^{10,11,13,14} Seidl *et al.*¹⁵ showed that also uniaxial strain can in principle be used to reduce the excitonic FSS. Due to the limited tuning range available, it has, however, remained unclear whether strain is suitable to reach sufficiently low values of FSS⁵ and what the mechanisms behind the observed FSS changes are. Based on atomistic model simulations for InGaAs/GaAs QDs, Singh and Bester¹⁹ predicted that uniaxial stress generally leads to an anticrossing of the bright excitonic states. Thereby, the magnitude and phase of the mixing of the bright excitonic states are modified, which results in a change of the FSS and in a rotation of the linear polarization of the emitted photons.¹⁸ Such an anticrossing behavior has been recently observed for QDs under strong vertical electric fields.¹³

Here we present the first experimental proof of the predictions in Ref. 18 for three different kinds of QDs under anisotropic biaxial stress. A continuum model based on eight-band $k \cdot p$ and configuration interaction theory qualitatively reproduces the observations, highlights their physical origin,

and shows how the minimum reachable FSS depends on the angle between strain axis and dot orientation.

The measurements are performed on two different samples grown by solid-source molecular beam epitaxy (MBE). The active structures consist of QDs embedded in thin membranes, which are released from the underlying substrate and transferred onto a piezoelectric actuator. The first membrane sample, with total thickness of about 150 nm, contains GaAs/AlGaAs QDs²³ and quantum well (QW) potential fluctuations (QWPFs).^{20,23} The latter, which are produced by local thickness or alloy fluctuations in a narrow QW, act as QDs with low confinement potential. The second sample contains standard InGaAs/GaAs QDs embedded in 200-nm-thick membranes.²⁴

The external stress is applied using a piezoelectric [Pb(Mg_{1/3}Nb_{2/3})O₃]_{0.72} – [PbTiO₃]_{0.28} (PMN-PT) crystal. By applying a voltage V between the front and the back surface of the crystal [i.e., along the x axis in Fig. 1(b)] the side faces, such as the top x - y plane, expand (or contract) parallel to the direction of the electric field F , for positive (negative) applied voltage. Simultaneously, the side faces contract (or expand) perpendicular to the electric field [i.e., along the y axis in Fig. 1(b)]. We denote the strain parallel to the x and y axes as ε and ε_\perp , respectively. The relation between these strain components is $\varepsilon_\perp \approx -0.7 \times \varepsilon$ (see Ref. 25). By placing membranes with QDs on the side faces of the PMN-PT we can thus apply strongly anisotropic biaxial stress on the QDs. According to previous results,^{16,26} we expect values of ε of the order of a few ‰ in the explored range of the electric field F . Photoluminescence (PL) spectroscopy measurements are performed at a temperature of 8 K in a standard micro-PL setup with a spectral resolution of about 70 μeV . The linear polarization of the luminescence is analyzed by combining a rotatable achromatic half-wave plate and a fixed linear polarizer.²⁴

Figure 1(a) shows a color-coded PL-intensity map for a neutral exciton (X) confined in a GaAs/AlGaAs QWPF as a function of the emission energy and polarization angle for different values of the electric field F applied to the PMN-PT

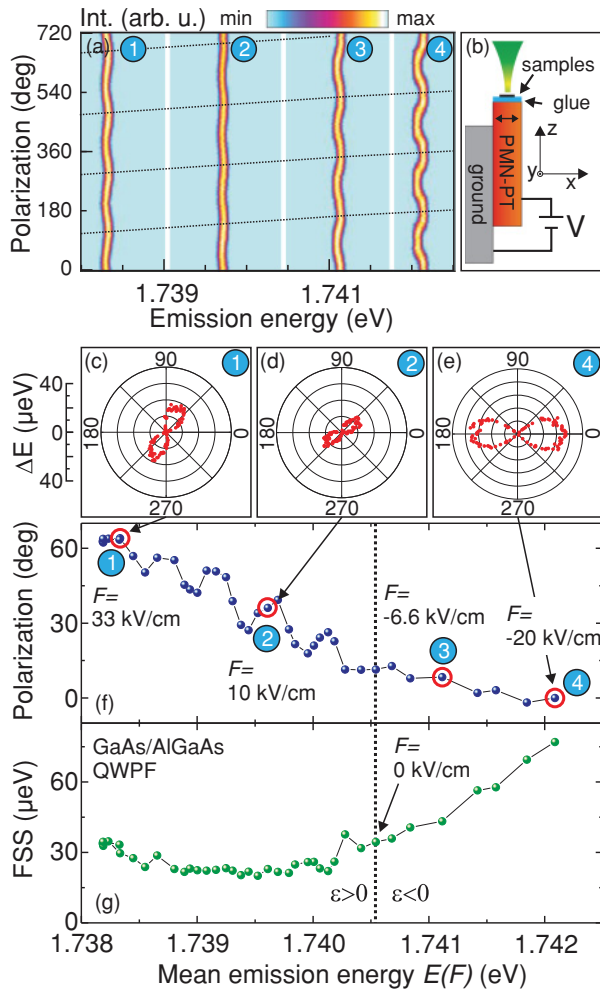


FIG. 1. (Color online) Behavior of a neutral exciton confined in a GaAs/AlGaAs QWPF under anisotropic biaxial stress. (a) Color-coded PL intensity vs polarization angle and energy for different values of electric fields applied to the piezoelectric actuator [the field values for the panels 1–4 are indicated in (f)]. The dashed lines are guides for the eye showing the rotation of the polarization direction. The x direction in (b) corresponds to polarization angles of 0° , 180° , 360° , 540° , and 720° and coincides with the polarization direction of the high-energy component of X at $F = -20$ kV/cm (panel 4). (b) Sketch of the device consisting of a membrane (sample) glued on a side of a PMN-PT crystal. (c),(d),(e) Polarization dependence in polar coordinates of the relative emission energy for panels 1, 2, and 4, respectively, of (a). The mean emission energy $E(F)$ for each value of F is subtracted. (f) Polarization angle of the high-energy component of X with respect to the direction of the electric field vs $E(F)$. The dots marked by red circles correspond to the data shown in (a). (g) FSS vs average emission energy.

(panels 1–4: $F = 33$, 10 , -6.6 , and -20 kV/cm). In this membrane the electric field direction forms an angle of about 20° with the $[1\bar{1}0]$ GaAs crystal direction. The periodic energy shift (wavy pattern) observed in PL is ascribed to the excitonic FSS (see, e.g., Ref. 23).

Two striking features clearly emerge from Fig. 1(a): (i) The polarization direction of the excitonic emission, related to the phase of the wavy pattern, rotates by more than 60° when F is changed from 33 to -20 kV/cm (see dotted lines); (ii) the

magnitude of the FSS, that is, the amplitude of the oscillations of the wavy patterns, first decreases and then increases with decreasing electric field. To extract quantitative information from the data, we first fit the peak position with a single Lorentzian curve at each polarization angle. The obtained relation of peak position E vs polarization angle ϕ is then fitted by a sine function to estimate both the magnitude of the FSS and the polarization of the X transitions with respect to the field direction [x axis in Fig. 1(b)]. The resolution in the determination of the FSS with this procedure is around $2.5 \mu\text{eV}$.²⁷ For FSS values larger than $10 \mu\text{eV}$, the uncertainty in the determination of the polarization direction is less than 10° .

Figures 1(c)–1(e) show polar plots of the relative peak positions $\Delta E = |E(\phi, F) - E(F)|$ extracted from Fig. 1(a) after subtraction of the average emission energy $E(F)$ measured for different values of F . The data, which are averaged over two periods of the polarization-resolved measurements (from 0° to 360° and from 360° to 720°), clearly show the strain-induced changes both in polarization direction and FSS. Figure 1(f) shows the orientation of the linear polarization of the high-energy component of X (with respect to the direction of F) as a function of $E(F)$. Figure 1(g) shows the corresponding behavior of the FSS. When moving from low to high emission energies, that is, from tensile to compressive strain along x , the FSS goes through a broad minimum before increasing again. The maximum observed change of the FSS for this QWPF is about $50 \mu\text{eV}$. Concerning the polarization direction we observe that: (i) It shows oscillations (with amplitude larger than the experimental uncertainty) superimposed to a smooth decrease when the FSS is minimum; (ii) It appears to saturate with increasing FSS and, more precisely, it is aligned parallel to F for strong compression (point 4). By performing similar measurements on different QWPFs we consistently observe the same qualitative behavior: The polarization rotation mainly occurs in correspondence to the minimum of the FSS. Interestingly, the minimum value of the FSS varies from one QWPF to another. Examples where the minimum FSS reaches values below about $5 \mu\text{eV}$ are presented in Fig. 2(d) and in the supplemental information.²⁴

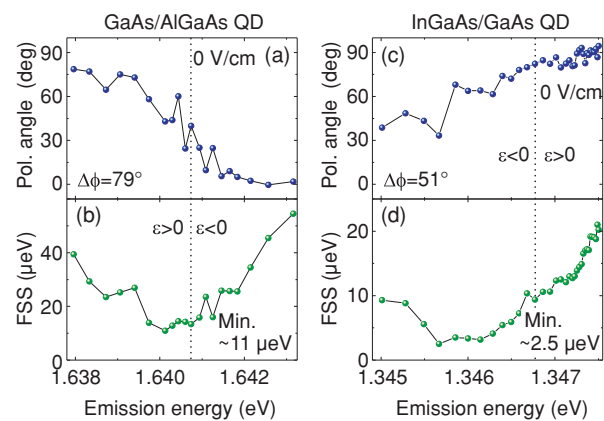


FIG. 2. (Color online) (a),(b) Polarization and FSS behavior of a GaAs/AlGaAs QD and (c),(d) of an InGaAs/GaAs QD. The polarization angle ϕ is defined as the angle of the higher energetic emission line with respect to the x direction in Fig. 1(b). For both QDs shown here the x direction roughly corresponds to the $[1\bar{1}0]$ direction of the GaAs membrane.

In order to test whether these effects occur also for other QD structures, we have performed measurements on GaAs/AlGaAs QDs and InGaAs/GaAs QDs (see Fig. 2).

For compressive strain, the emission energy of the GaAs/AlGaAs QD presented in Figs. 2(a) and 2(b) blueshifts similar to the QWPFs, whereas the emission energy of the presented InGaAs/GaAs QD [Figs. 2(c) and 2(d)] redshifts. The fact that a redshift is observed for the InGaAs QD is in qualitative agreement with the calculations presented in Ref. 19 for In-rich QDs. In spite of the very different structural properties and behavior of the emission energy under anisotropic strain, the excitonic behavior of the two different types of QDs is qualitatively the same as for the GaAs/AlGaAs QWPFs: we observe a clear polarization rotation of the emitted light (by 79° for the GaAs/AlGaAs QD and by 51° for the InGaAs/GaAs QD) [see Figs. 2(a) and 2(c)]. Simultaneously, the FSS is tuned in a range of $\sim 70 \mu\text{eV}$ for the GaAs QD and $\sim 25 \mu\text{eV}$ for the InGaAs QD [see Figs. 2(b) and 2(d)]. Furthermore, the rotation of the polarization mainly takes place when the FSS reaches its minimum value.

The above findings are consistent with a strain-induced anticrossing of the bright states of a neutral exciton, which was recently predicted by Singh and Bester for InGaAs QDs¹⁹ via atomistic model simulations. In order to gather more insight on the physical origin of the observed phenomena, we calculate the excitonic FSS of model dots by combining the eight-band $k \cdot p$ model and the configuration interaction method following the approach described in Refs. 28, 29, and 23. Strain is introduced via the Pikus-Bir Hamiltonian.³⁰ In the model we consider a semiellipsoidal GaAs/AlGaAs QD with composition equal to the nominal one used in the experiment. The main axis ε of the anisotropic biaxial strain [x axis in Fig. 1(b)] coincides with the $[1\bar{1}0]$ GaAs crystal direction and we assume $\varepsilon_\perp \approx -0.7 \times \varepsilon$ [see insets in Fig. 3(b)]. The main axis of the QD forms an angle α with respect to the $[110]$ direction [see right inset in Fig. 3(a)].²⁴

Figures 3(a) and 3(b) show, for different values of α , the calculated polarization angle and the FSS as a function of ε , respectively. We begin with the ideal situation of a QD elongated along the $[110]$ crystal direction ($\alpha = 0$). For zero strain, the QD has a FSS of $33 \mu\text{eV}$, which is comparable with typical observed values. When the QD is stretched, both exciton transitions remain linearly polarized and perpendicular to each other (not shown) and the FSS varies in a wide range [see Fig. 3(b)]. For a strain ε of 0.086% the FSS reaches its minimum value below $0.4 \mu\text{eV}$. The polarization direction of the high-energy component, shown in Fig. 3(a), is perpendicular to the elongation direction of the QD for strains below 0.086% and abruptly changes by 90° for higher strains.

For increasing α , the polarization direction varies in a wider range of strain values; that is, it rotates smoothly as a function of strain, as shown in Fig. 3(a). Correspondingly, the minimum of the FSS becomes increasingly broad and the reached minimum value increases with increasing α . We also note that at zero strain the polarization angle is determined by the orientation of the dot. As the strain increases, the structural orientation becomes less important and the polarization angle is determined mostly by the magnitude and direction of the strain, yielding similar values for all dot orientations. This behavior is also observed in the experiments: For the largest

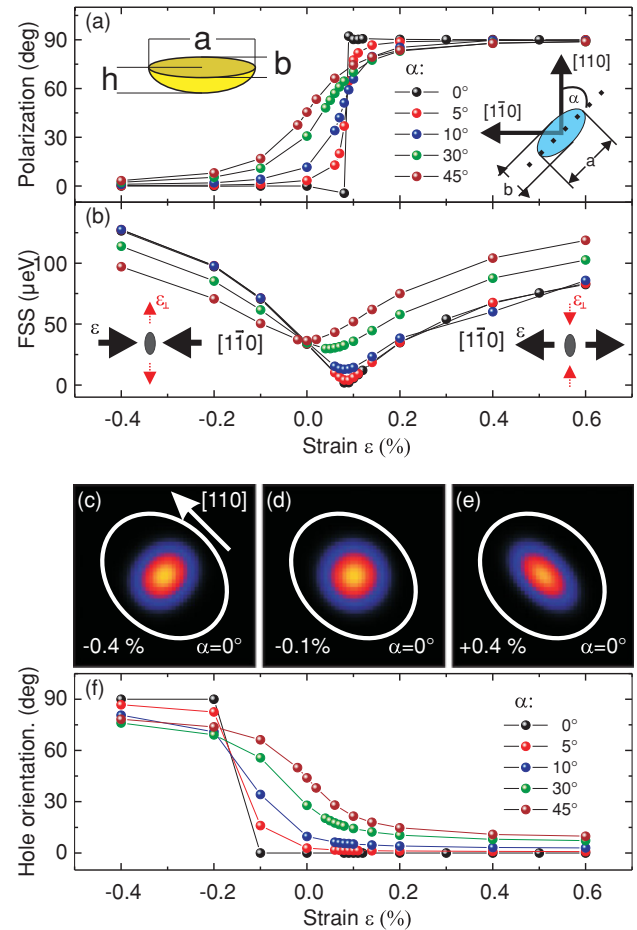


FIG. 3. (Color online) Theoretical study of the influence of anisotropic biaxial strain on the light emitted by a excitons in model GaAs/AlGaAs QDs. The left inset in (a) shows the shape of the artificial structure. (a) Polarization of the high-energy excitonic component with respect to the x direction ($[1\bar{1}0]$) in Fig. 2(b) for different values of α (i.e., angle of the elongation direction with respect to the $[110]$ crystal direction; see right inset). (b) Corresponding values of the FSS, the left (right) inset displays the direction of the applied stress for compressive (tensile) strains ε . (c)–(e) Density map of the ground-state hole wave function for a QD with $\alpha = 0$ for different strain values. The white ellipse indicates the shape of the QD. (f) Orientation of the hole wave function with respect to the $[110]$ direction vs strain. See text for more details.

available strains, and away from the FSS minimum, anisotropic biaxial stress allows us to orient the polarization direction parallel/perpendicular to the strain direction in a predictable way [see Figs. 1(a)–1(e)]. Finally we note that similar results are obtained when the direction of the strain is changed and the QD is kept fixed instead of rotating the QD shape with respect to the crystal direction as discussed here.²⁴

By inspecting the single-particle states we found that small strains produce relevant changes on the ground-state hole wave function, while their effect on the electron wave function is much weaker. In particular: (i) The proportion of the light hole band in the hole state is substantially increased (e.g., from 0.6% at $\varepsilon = 0\%$ to 11% at $\varepsilon = 0.2\%$ for $\alpha = 0$); (ii) the hole wave function changes in shape and orientation, as illustrated in Figs. 3(c)–3(e) for $\alpha = 0$. In general, for finite

values of α , the elongation direction of holes rotates by up to 90° , as shown in Fig. 3(f). At the same time the electron wave function rotates by $<7^\circ$ (not shown). These effects are a consequence of the nondiagonal terms in the Pikus-Bir Hamiltonian, which enhance the mixing of the heavy hole band with other bands (in particular, the light hole band) and modify the effective mass causing its pronounced anisotropy along the principal stress axes $[110]$ and $[1\bar{1}0]$. The smooth rotation of the hole wave function observed for finite values of α [see Fig. 3(f)], which is analogous to the behavior observed for the polarization direction [see Fig. 3(a)], is due to the joined influence of the structural anisotropy (elongation of the QD) and the anisotropy of the effective mass, which tends to elongate the wave functions along the $[110]$ or $[1\bar{1}0]$ direction depending on the sign of the applied strain. We note that the effects of the strain-induced band edge shift and the created piezoelectric potential on the FSS are negligible.

In spite of the simplicity of the model QD shape, the presented continuum model is able, for finite values of α , to account for the experimental observations

In conclusion, we have reported on the effects of anisotropic biaxial stress on the emission of neutral excitons confined

in single semiconductor QDs. We have shown that relatively small strains are sufficient to produce dramatic changes of the polarization direction and of the energy splitting of the excitonic exchange-split doublet. Qualitatively the same results are obtained from three different kinds of QDs, consistent with a scenario involving a strain-induced anticrossing of the bright excitonic states.¹⁹ Based on a continuum model, which is able to reproduce the main observed features, we ascribe the effects to substantial changes of the hole states. The theoretical investigation also shows that, for a given QD structure, the minimum reachable FSS depends strongly on the direction of the strain.

We acknowledge V. Fomin, S. Kiravittaya, P. Atkinson, T. Zander, R. Trotta, G. Bester, R. Singh, and C. C. Bof Bufon for fruitful discussions and technical support. V.K. and P.K. were supported by Institutional research program MSM 0021622410 and the GACR Grant No. GA202/09/0676. The calculations were partly performed on grid Wiggum (TU-Berlin) using the software package dotkp. This work was supported by the DFG (FOR730 and SFB 787) and the BMBF (QK_QuaHL-Rep, 01BQ1032).

*j.d.plumhof@ifw-dresden.de

†a.rastelli@ifw-dresden.de

¹S. M. de Vasconcellos, S. Gordon, M. Bichler, T. Meier, and A. Zrenner, *Nat. Photon.* **4**, 545 (2010).

²D. Press, T. D. Ladd, B. Zhang, and Y. Yamamoto, *Nature (London)* **456**, 218 (2008).

³D. Brunner, B. D. Gerardot, P. A. Dalgarno, G. Wüst, K. Karrai, N. G. Stoltz, P. M. Petroff, and R. J. Warburton, *Science* **325**, 70 (2009).

⁴N. Akopian, N. H. Lindner, E. Poem, Y. Berlatzky, J. Avron, D. Gershoni, B. D. Gerardot, and P. M. Petroff, *Phys. Rev. Lett.* **96**, 130501 (2006).

⁵A. J. Hudson, R. M. Stevenson, A. J. Bennett, R. J. Young, C. A. Nicoll, P. Atkinson, K. Cooper, D. A. Ritchie, and A. J. Shields, *Phys. Rev. Lett.* **99**, 266802 (2007).

⁶R. Hafenbrak, S. M. Ulrich, P. Michler, L. Wang, A. Rastelli, and O. G. Schmidt, *New J. Phys.* **9**, 315 (2007).

⁷A. Dousse, J. Suffczynski, A. Beveratos, O. Krebs, A. Lemaitre, I. Sagnes, J. Bloch, P. Voisin, and P. Senellart, *Nature (London)* **466**, 217 (2010).

⁸S. Empedocles and M. Bawendi, *Science* **278**, 2114 (1997).

⁹M. Bayer, G. Ortner, O. Stern, A. Kuther, A. A. Gorbunov, A. Forchel, P. Hawrylak, S. Fafard, K. Hinzer, T. L. Reinecke, S. N. Walck, J. P. Reithmaier, F. Klopff, and F. Schäfer, *Phys. Rev. B* **65**, 195315 (2002).

¹⁰B. D. Gerardot, S. Seidl, P. A. Dalgarno, R. J. Warburton, D. Granados, J. M. Garcia, K. Kowalik, O. Krebs, K. Karrai, A. Badolato, and P. M. Petroff, *Appl. Phys. Lett.* **90**, 041101 (2007).

¹¹M. M. Vogel, S. M. Ulrich, R. Hafenbrak, P. Michler, L. Wang, A. Rastelli, and O. G. Schmidt, *Appl. Phys. Lett.* **91**, 051904 (2007).

¹²R. Stevenson, R. Young, P. Atkinson, K. Cooper, D. Ritchie, and A. Shields, *Nature (London)* **439**, 179 (2006).

¹³A. J. Bennett, M. A. Pooley, R. M. Stevenson, M. B. Ward, R. B. Patel, A. Boyer de la Giroday, N. Sköld, I. Farrer, C. A. Nicoll, D. A. Ritchie, and A. J. Shields, *Nat. Phys.* **6**, 947 (2010).

¹⁴I. E. Itskevich, S. G. Lyapin, I. A. Troyan, P. C. Klipstein, L. Eaves, P. C. Main, and M. Henini, *Phys. Rev. B* **58**, 4250 (1998).

¹⁵S. Seidl, M. Kroner, A. Hoge, K. Karrai, R. Warburton, A. Badolato, and P. Petroff, *Appl. Phys. Lett.* **88**, 203113 (2006).

¹⁶F. Ding, R. Singh, J. D. Plumhof, T. Zander, V. Křápek, Y. H. Chen, M. Benyoucef, V. Zwiller, K. Dörr, G. Bester, A. Rastelli, and O. G. Schmidt, *Phys. Rev. Lett.* **104**, 067405 (2010).

¹⁷M. Metcalfe, S. M. Carr, A. Muller, G. S. Solomon, and J. Lawall, *Phys. Rev. Lett.* **105**, 037401 (2010).

¹⁸G. W. Bryant, M. Zielinski, N. Malkova, J. Sims, W. Jaskólski, and J. Aizpurua, *Phys. Rev. Lett.* **105**, 067404 (2010).

¹⁹R. Singh and G. Bester, *Phys. Rev. Lett.* **104**, 196803 (2010).

²⁰D. Gammon, E. S. Snow, B. V. Shanabrook, D. S. Katzer, and D. Park, *Phys. Rev. Lett.* **76**, 3005 (1996).

²¹H. Y. Ramirez, C. H. Lin, C. C. Chao, Y. Hsu, W. T. You, S. Y. Huang, Y. T. Chen, H. C. Tseng, W. H. Chang, S. D. Lin, and S. J. Cheng, *Phys. Rev. B* **81**, 245324 (2010).

²²O. Benson, C. Santori, M. Pelton, and Y. Yamamoto, *Phys. Rev. Lett.* **84**, 2513 (2000).

²³J. D. Plumhof, V. Křápek, L. Wang, A. Schliwa, D. Bimberg, A. Rastelli, and O. G. Schmidt, *Phys. Rev. B* **81**, 121309(R) (2010).

²⁴See supplemental material at [<http://link.aps.org/supplemental/10.1103/PhysRevB.83.121302>] for expanded data.

²⁵M. D. Biegalski, K. Dörr, D. H. Kim, and H. M. Christen, *Appl. Phys. Lett.* **96**, 151905 (2010).

²⁶T. Zander, A. Herklotz, S. Kiravittaya, M. Benyoucef, F. Ding, P. Atkinson, S. Kumar, J. D. Plumhof, K. Dörr, A. Rastelli, and O. G. Schmidt, *Opt. Express* **17**, 22452 (2009).

²⁷F. Ding, N. Akopian, B. Li, U. Perinetti, A. Govorov, F. M. Peeters, C. C. Bof Bufon, C. Deneke, Y. H. Chen, A. Rastelli, O. G. Schmidt, and V. Zwiller, *Phys. Rev. B* **82**, 075309 (2010).

²⁸O. Stier, M. Grundmann, and D. Bimberg, *Phys. Rev. B* **59**, 5688 (1999).

²⁹T. Takagahara, *Phys. Rev. B* **62**, 16840 (2000).

³⁰G. E. Pikus and G. L. Bir, *Symmetry and Strain Induced Effects in Semiconductors* (Wiley, New York, 1974).